DOI: 10.7641/CTA.2017.16166

涡轮增压汽油机气路预测模型的建立与预测控制

陈 欢[1,2], 胡云峰[1,2†], 于树友[1,2], 孙鹏远[3], 陈 虹[1,2]

(1. 吉林大学 汽车仿真与控制重点实验室, 吉林 长春 130025;
2. 吉林大学 通信工程学院, 吉林 长春 130025; 3. 中国一汽集团公司研究设计中心, 吉林 长春 130011)

摘要: 针对涡轮增压汽油机气路系统中节气门与废气旁通阀动力学耦合、机理建模复杂的问题, 本文提出基于神经网络模型的气路系统预测控制方法，实现了节气门与废气旁通阀的协调控制. 首先, 针对涡轮增压汽油机气路系统map与机理混合描述的特性, 利用系统的输入输出数据，采用反向传播神经网络(back propagation neural network, BPNN)训练得到一个非线性气路模型; 其次, 基于泰勒展开式对预测模型进行线性化, 并对模型的精度进行了验证，进而利用该模型预测系统的未来动态; 然后, 在考虑系统存在输入约束的条件下, 设计了一个线性模型预测控制器对节气门与废气旁通阀进行协调控制, 实现了进气歧管压力和升压的跟踪控制进而满足发动机的扭矩需求; 最后, 通过离线仿真和基于dSPACE的快速原型实验(rapid control prototyping, RCP)验证了控制系统的有效性和实时性.

关键词: 涡轮增压汽油机控制; 模型预测控制; 预测模型; BP神经网络

中图分类号: TP273 **文献标识码**: A

Airpath prediction model and predictive control of turbocharged gasoline engine

CHEN Huan[1,2], HU Yun-feng[1,2†], YU Shu-you[1,2], SUN Peng-yuan[3], CHEN Hong[1,2]

(1. State Key Laboratory of Automotive Simulation and Control, Jilin University, Changchun Jilin 130025, China;
2. College of Communication Engineering, Jilin University, Changchun Jilin 130025, China;
3. China FAW Group Corporation Research and Design Center, Changchun Jilin 130011, China)

Abstract: In this paper, a neural network based model predictive controller is developed for the coordinated control of the throttle and wastegate in a turbocharged gasoline engine airpath system. Firstly, considering the mixed description of map and physical for engine airpath system, a data-driven nonlinear airpath model is trained using back propagation neural network (BPNN) to predict the future dynamics of the turbocharged engine. Secondly, the prediction model is linearized based on Taylor expansion and the feasibility of this simplification is assessed. Thirdly, in order to satisfy the engine torque demand, a linear model predictive controller is designed to manage the throttle and wastegate so that the engine tracks the setpoints of the intake manifold pressure and boost pressure considering the system constraints. Furthermore, simulation results are presented to verify the effectiveness of the controller. Finally, a rapid control prototyping (RCP) experiment based on dSPACE is further implemented to test the real-time performance.

Key words: turbocharged gasoline engine control; model predictive control; prediction model; BP neural network

1 Introduction

With the aggravation of energy crisis and the increasing issue of environmental pollution, the development of automobile industry is confronted with tremendous challenges. The turbo-charge technology is one of the promising methods to relieve this situation. This technology utilizes the energy of exhaust gas as the power of turbine, so as to increase the amount of air mass flow entering cylinders. Meanwhile, by increasing fuel mass flow correspondingly, the capacity of isovolumetric engines could be promoted, thus to satisfy people's demand for automotive power[1–2]. In addition, sufficient air makes for the combustion in the cylinders, which produces less harmful gas[3].

Nowadays, the torque-centered engine control scheme is widely applied to improve the engine control performance. Where, the driver's torque demand is translated to the tracking control of airpath system. Then, the model-based controller synthesis and analysis method are used for the airpath control of the turbocharged gasoline engine, where the intake manifold pressure and boost pressure are considered as control

Received 28 November 2016; accepted 11 May 2017.
†Corresponding author. E-mail: huyf@jlu.edu.cn; Tel.: +86 13756056375.
Recommended by Associate Editor TAN Yonghong.
Supported by National Natural Science Foundation of China (61703177，61520106008), Jilin Provincial Science and Technology Department Project (20170520067JH) and Jilin Provincial Education Department Project (JJKH20170801KJ).

output, the throttle and wastegate are considered as control input[4–5]. Hence, a precise control-oriented model is essential for control design. There are two groups of modeling method. The first group is physical modeling method: a nonlinear physical model with maps is established in [6–7], and a switching Takagi-Sugeno (T–S) model is proposed in [8–9]. The second group is model identification method: a data-driven model based on subspace identification is proposed in [10], where the least-square method is utilized to construct predictive equation. According to certainty equivalence principle, the linear model and inverse model of turbo engine are identified respectively in [11]. Based on the above models, the control scheme can be roughly classified into three categories. The first category is single input single output (SISO) control method which only adjusts the wastegate to track the desired boost pressure, where the throttle is considered as an exogenous input. A linear model predictive control (MPC) is used in [12] to control the wastegate to track the desired boost pressure. A composite adaptive internal model control (CAIMC) method based on linear identified model is proposed in [11] to achieve the desired boost pressure. An internal model control (IMC) based on quasi-LPV model is designed in [13]. The realization of this method is simple. However, it ignores the influence of other interrelated controller which adjusts throttle to track air mass flow entering cylinders, the influence of other interrelated controller may be an uncertain factor to destroy the control performance. The second category is two input single output (TISO) control method, which considers the overall actuators (throttle and wastegate) as control input, and considers the air mass flow entering cylinders or intake manifold pressure as control output. IMC and MPC are utilized to control the throttle and wastegate coordinately in [14] to track the desired air mass flow entering cylinders. In order to reduce the influence of time-delay, modeling uncertainties and the bounded measurement noises, a switching robust H_∞ controller based on switching T–S model is proposed in [8] to track desired intake manifold pressure. The multi-objective control method is applied to track the desired intake manifold pressure in [9]. Although this category can meet the driver's torque demand, the boost pressure is not considered in the control scheme, which will lead to the problems like cylinder knocking and pumping loss enlarging in the overlarge boost pressure condition. The third category is two input two output (TITO) control method, where the throttle and wastegate are adjusted to achieve the desired intake manifold pressure (or air mass flow entering cylinders) and the desired boost pressure. A distributed control method is proposed in [15]. This method ignores the coupling effects of the throttle and wastegate in the airpath system, which are controlled to track intake manifold pressure and boost pressure separately. A linear model predictive controller is designed in [16] for the coordinated control of the turbocharged engine, the authors deduce a state equation consists of five state variables as the prediction model, which contains unmeasurable state variables, and the workload of on-line computation is also increased. MPC can deal with the coupling effects of the throttle and wastegate effectively, and can directly consider the constraint in the optimization process[17].

Although MPC is suitable for turbocharged engine control, it is difficult to build a precise physical model because of the existence of the dynamic coupling and maps (volumetric efficiency map, compressor isentropic efficiency map etc) in practical process[7]. Recently, neural network is widely used to obtain model via input-output data without any knowledge of system dynamics[18–19]. The neural network is utilized for fault-detection of engine in [20–21], for modeling the effect of the variable valve timing (VVT) in [22], for the prediction of the engine performance in [23–24].

In this paper, a neural network based predictive controller is developed to deal with the coordinated control of turbocharged engine airpath system. The main merits are as follows:

1) A nonlinear data-based airpath model is deduced using BP neural network method. Then, a linear prediction model is obtained by Taylor expansion to predict future dynamics. This model only has two measurable state variables, which can reduce the workload of online calculation;

2) A linear model predictive controller is developed for turbocharged engine airpath system, the tracking control of the intake manifold pressure and boost pressure is considered in the objective function, the limitation of throttle and wastegate angles is considered as input constraint. Then, the optimization problem is solved by quadratic programming;

3) The simulation results and rapid control prototyping experiment are presented to verify the effectiveness and real-time performance of the system under control.

The structure of this paper is as follows. Section II states the turbocharged gasoline engine system and overall control scheme. A BP neural network based predictive model is trained in Section III. In Section IV, a detail designed procedure of the linear neural network predictive controller is proposed. The simulation results to verify the effectiveness of the proposed controller are shown in Section V. Section VI presents the rapid control prototyping platform experiment results. Finally, the conclusion is drawn in Section VII.

2 Problem description

The structure of the turbocharged gasoline engine is shown in Fig. 1. The throttle and wastegate are the main actuators to track the intake manifold pressure and the boost pressure. The degrees of wastegate and the amount of exhaust gas jointly control the boost pressure

by changing turbine rotational speed. Then, the compressed air passes through an intercooler and a throttle. Before the air goes into cylinders, the intake manifold pressure could be changed by throttle.

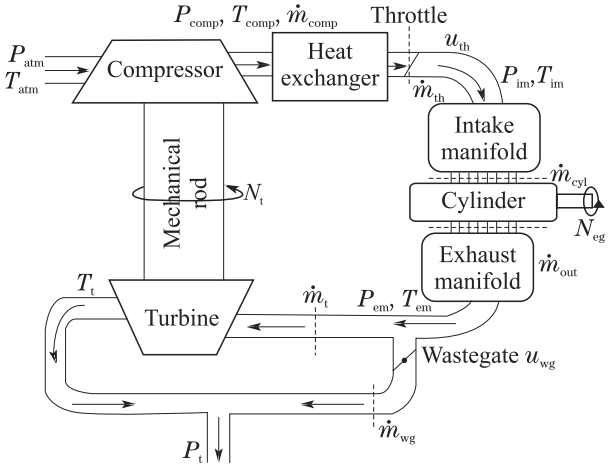

Fig. 1 Structure of a turbocharged gasoline engine

The two actuators and two pressures are coupled to each other and the engine system contains maps. All of those cause the difficulties of obtaining physical model and designing controller. Moreover, many engine researches take decentralized control method to deal with the TITO control problem, which ignore the coupling between them. Hence, the BPNN based MPC scheme is employed to coordinate the throttle and wastegate in this paper. The overall control scheme is shown in Fig. 2. According to different engine speed, the desired torque is converted into the desired intake manifold pressure and the boost pressure by maps as shown in Figs. 3−4. Then, the two desired pressures are tracked by controlling the throttle and wastegate. Furthermore, BPNN is applied to identify the turbocharged gasoline engine so as to get the predictive model. Due to the heavy computational burden of nonlinear MPC, the BPNN based linear MPC is adopted. TDL is the time-delay line. On-line correction is used to compensate the error of model mismatch.

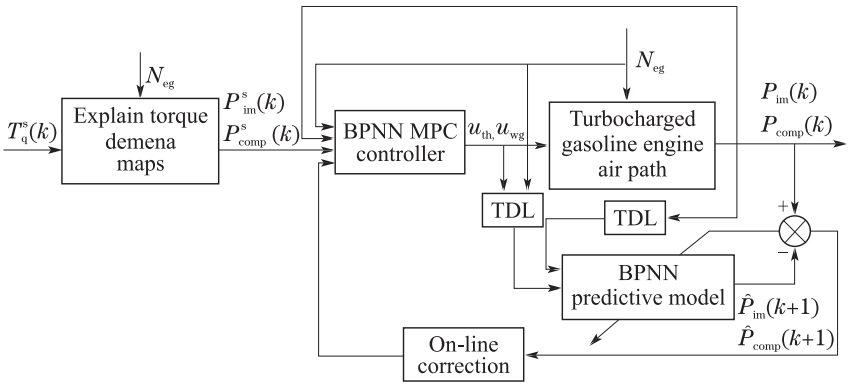

Fig. 2 The control scheme of engine air path system

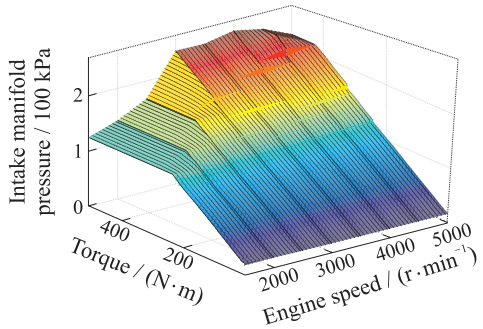

Fig. 3 Torque demand converted into intake manifold pressure map

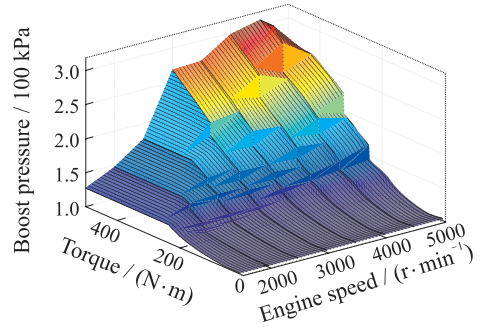

Fig. 4 Torque demand converted into boost pressure map

To obtain the input-output relationships of BPNN, we need to get enough reliable training samples. Therefore, a high-precision turbocharged gasoline engine model of the commercial software LMS Imagine. Lab AMESim Rev 13 (AMESim) is taken as the plant.

3 BPNN predictive model

Neural network is a mathematical model of imitating human brain structure and behavior. In the past few decades, a wide variety of neural networks are poured into research, such as BPNN, radial basis function (RBF) neural network, hopfield neural network and so on. Among all of them, hopfield neural network is a kind of feedback neural network which is usually adopted to mathematical optimization. BPNN and RBF neural network are most widely used in system identification. RBF neural network is a kind of local approximation network which is adequate for on-line learning. BPNN is a global network which could work better for the off-line identification

of complex system. Since the airpath system is a two input two output nonlinear system and the computational burden of MPC is heavy, the on-line identification method can't satisfy the demand of real-time performance. Hence, the method of off-line identification is adopted in this paper. BPNN consists of an input layer, one or more hidden layers and an output layer. There are full of interconnections among the neurons in different layers and no connection among neurons in the same layer. In the process of identification, as long as it has a sufficient number of hidden layers and hidden neurons, in principle it can approximate any nonlinear system with the given accuracy[25].

In practical application, there is no good way to select the number of hidden layers and hidden layer neurons[26]. BPNN predictive model will be linearized in next section to guarantee the real-time performance. Hence, the number of hidden layers and hidden layer neurons have no influence on the real-time of controller. Therefore, according to the characteristics of turbocharged gasoline engine and experiments, we design a four-layer neural network whose neurons have no threshold as shown in Fig. 5. In this paper, input layer and output layer take purlin function as the activation function, and hidden layers use the sigmoid function.

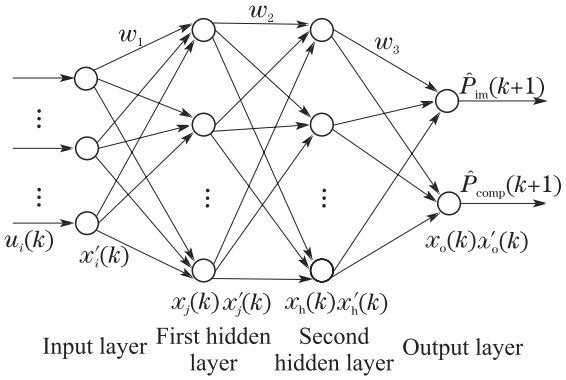

Fig. 5 The structure of BP neural network

The number of input layer neurons is the same as the amount of system input, and the output of the input layer is

$$x'_i = u_i. \tag{1}$$

The input and output of the first hidden layer are

$$x_j = \sum_{i=1}^{I} w_1(j,i)x'_i, \tag{2a}$$

$$x'_j = \frac{1}{1+\mathrm{e}^{-x_j}}, \tag{2b}$$

where I is the number of input layer neurons, and w_1 represents the weights between input layer and the first hidden layer.

The input and output of the second hidden layer neurons can be represented as

$$x_{\rm h} = \sum_{j=1}^{J} w_2(h,j)x'_j, \tag{3a}$$

$$x'_{\rm h} = \frac{1}{1+\mathrm{e}^{-x_{\rm h}}}, \tag{3b}$$

where J is the number of the first hidden layer neurons, and w_2 stands for the weights between hidden layers.

The input and output of the output layer can be represented as:

$$x_{\rm o} = \sum_{h=1}^{H} w_3(o,h)x'_{\rm h}, \tag{4a}$$

$$x'_{\rm o} = x_{\rm o}, \tag{4b}$$

where H is the number of the second hidden layer neurons, and w_3 is the weights between the second hidden layer and output layer.

In terms of general system, the system output is related to its input, disturbance and the pass values of output. As in the research of turbocharged engine air path control, the intake manifold pressure $P_{\rm im}$ and boost pressure $P_{\rm comp}$ are connected with the throttle $u_{\rm th}$, the wastegate $u_{\rm wg}$ and the engine speed $N_{\rm eg}$, where, $u_{\rm th}$ and $u_{\rm wg}$ are the input variables of turbocharged engine air path system, and $N_{\rm eg}$ is the state variable. Since $N_{\rm eg}$ is a slow state variable which is measured, we take it as a disturbance. Therefore, the selected input variables and their orders of BPNN model are shown in Fig. 6, where m and n stand for the orders of engine model input and output variables respectively. $\hat{P}_{\rm im}(k)$ and $\hat{P}_{\rm comp}(k)$ are predicted values of the intake manifold pressure and boost pressure at sampling time k, which are predicted by BPNN model.

In BPNN implementation procedure, the training samples play an important role. To get a good identification result, we should choose a set of training samples which reflect the system dynamics. Therefore, the throttle degree $u_{\rm th}$, the wastegate degree $u_{\rm wg}$ and the engine speed $N_{\rm eg}$ are taken as the input to stimulate the engine plant, where the intake manifold pressure $P_{\rm im}$ and boost pressure $P_{\rm comp}$ are output. A group of input data which covers nearly entire working condition is shown in Fig. 7. Under the ideal air-fuel ratio, the input data acts on the AMESim turbocharged gasoline engine model to get the output data. The output curves are shown in Fig. 8.

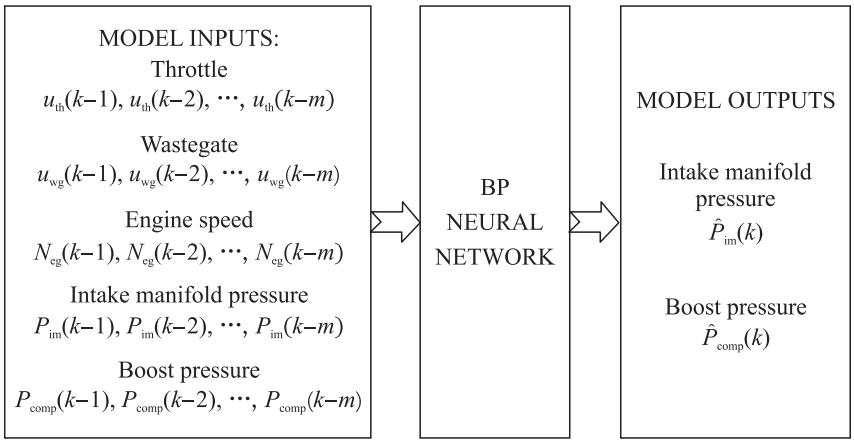

Fig. 6 The input-output of BPNN

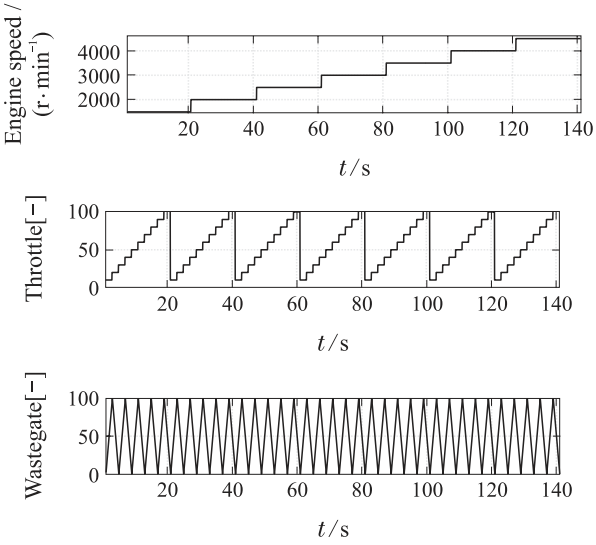

Fig. 7 Input data for stimulation

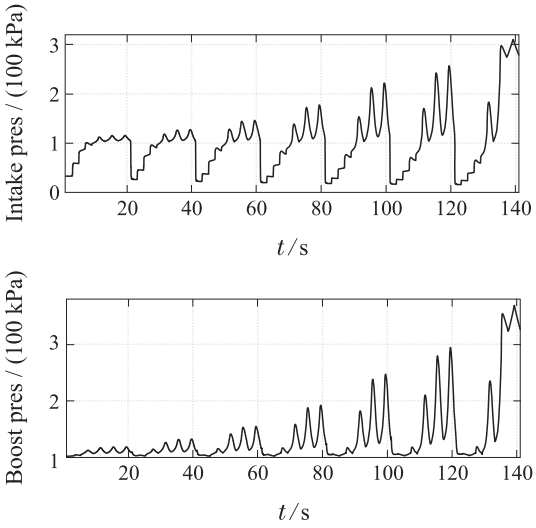

Fig. 8 Output data for stimulation

We train BPNN model by BPNN toolbox of MATLAB. All of the input-output data of the BPNN model are normalized to avoid the singular points which are caused by the large gap orders of magnitude among inputs.

According to the structure of BPNN model and the trained weights, we can describe the BPNN system:

$$\begin{aligned}\hat{y}(k) = &\sum_{h=1}^{H} w_3([1,2],h)\cdot\\ &g\{\sum_{j=1}^{J} w_2(h,j)g[\sum_{i=1}^{m} w_1(j,i)N_{\rm eg}(k-i)+\\ &\sum_{i=m+1}^{2m} w_1(j,i)u_{\rm th}(k+m-i)+\\ &\sum_{i=2m+1}^{3m} w_1(j,i)u_{\rm wg}(k+2m-i)+\\ &\sum_{i=3m+1}^{3m+n} w_1(j,i)P_{\rm im}(k+3m-i)+\\ &\sum_{i=3m+n}^{I} w_1(j,i)P_{\rm comp}(k+3m+n-i)]\},\end{aligned} \tag{5}$$

where

$$\hat{y}(k) = \begin{bmatrix}\hat{P}_{\rm im}(k)\\ \hat{P}_{\rm comp}(k)\end{bmatrix},\ g(x) = \frac{1}{1+{\rm e}^{-x}}. \tag{6}$$

4 Model predictive control for turbo engine

In the theory of MPC, engine model is utilized to predict its future evolution. However, it is not easy to obtain a precise mechanism model due to the complexity of the system. Therefore, neural network identification is used to obtain the predictive model via input-output data in this paper. BPNN based MPC integrates model predictive control with BP neural network identification method. On the basis of above research about BPNN model, a linear MPC will be designed in next work.

Almost all systems are nonlinear. Thanks to the sigmoid function, the BPNN model we trained is a nonlinear model too. Due to the complex optimization of nonlinear MPC, the real-time performance of

it can not be guaranteed. Hence, a linear MPC is deduced by Taylor expansion, where a bit control precision must be sacrificed.

4.1 Predictive equation

4.1.1 The linearisation of BPNN model

This BPNN model can be directly used in nonlinear MPC. In order to reduce the heavy computational burden, Taylor expansion is utilized to linearize the BPNN model. Set $s_{3h}(k)$ and $s_{2j}(k)$:

$$\begin{cases} s_{2j}(k) = \sum\limits_{i=1}^{m} w_1(j,i) N_{\mathrm{eg}}(k-i) + \\ \quad \sum\limits_{i=m+1}^{2m} w_1(j,i) u_{\mathrm{th}}(k+m-i) + \\ \quad \sum\limits_{i=2m+1}^{3m} w_1(j,i) u_{\mathrm{wg}}(k+2m-i) + \\ \quad \sum\limits_{i=3m+1}^{3m+n} w_1(j,i) P_{\mathrm{im}}(k+3m-i) + \\ \quad \sum\limits_{i=3m+n}^{I} w_1(j,i) P_{\mathrm{comp}}(k+3m+n-i), \\ s_{3h}(k) = \sum\limits_{j=1}^{J} w_2(h,j) g[s_{2j}(k)]. \end{cases} \tag{7}$$

Expand the predictive equation on centers s_{3h} $(h=1,\cdots,H)$ and s_{2j} $(j=1,\cdots,J)$, respectively, to get an expanded equation:

$$\hat{y}(k) = \sum_{h=1}^{H} w_3([1,2],h) \sum_{j=1}^{J} M_j s_{2j}(k) + N + \theta(k), \tag{8}$$

where

$$\begin{cases} M_j = w_2(h,j) g'(s_{3h}) g'(s_{2j}), \\ N = \\ \sum\limits_{h=1}^{H} w_3([1,2],h) \{ \sum\limits_{j=1}^{J} w_2(h,j) g'(s_{3h}) [g(s_{2j}) - \\ g'(s_{2j}) s_{2j}] + g(s_{3h}) - g'(s_{3h}) s_{3h} \}. \end{cases} \tag{9}$$

The term $\theta(k)$ in Eq.(8) is the nonlinear part, and could be ignored in linear predictive equation. Since discrete difference equation simplifies the whole formula derivation procedure, it is necessary to vary the Eq.(8) to a discrete difference equation:

$$\begin{aligned} &\hat{y}(k) = \\ &a_1 y(k-1) + \cdots + a_n y(k-n) + \\ &b_1 N_{\mathrm{eg}}(k-1) + b_m N_{\mathrm{eg}}(k-m) + \cdots + \\ &b_{m+1} u_{\mathrm{th}}(k-1) + \cdots + b_{2m} u_{\mathrm{th}}(k-m) + \\ &b_{2m+1} u_{\mathrm{wg}}(k-1) + \cdots + b_{3m} u_{\mathrm{wg}}(k-m) + N, \end{aligned} \tag{10}$$

where

$$\begin{cases} a_x = \begin{bmatrix} a_{\mathrm{t}x} & a_{\mathrm{tc}x} \\ a_{\mathrm{ct}x} & a_{\mathrm{c}x} \end{bmatrix}, \ x = 1, \cdots, n, \\ b_z = \begin{bmatrix} b_{\mathrm{t}z} \\ b_{\mathrm{c}z} \end{bmatrix}, \ z = 1, \cdots, 3m, \\ a_{\mathrm{t}x} = \sum\limits_{h=1}^{H} w_3(1,h) \sum\limits_{j=1}^{J} M_j w_1(j, 3m+x), \\ a_{\mathrm{tc}x} = \sum\limits_{h=1}^{H} w_3(1,h) \sum\limits_{j=1}^{J} M_j w_1(j, 3m+n+x), \\ a_{\mathrm{ct}x} = \sum\limits_{h=1}^{H} w_3(2,h) \sum\limits_{j=1}^{J} M_j w_1(j, 3m+x), \\ a_{\mathrm{c}x} = \sum\limits_{h=1}^{H} w_3(2,h) \sum\limits_{j=1}^{J} M_j w_1(j, 3m+n+x), \\ b_{\mathrm{t}z} = \sum\limits_{h=1}^{H} w_3(1,h) \sum\limits_{j=1}^{J} M_j w_1(j,z), \\ b_{\mathrm{c}z} = \sum\limits_{h=1}^{H} w_3(2,h) \sum\limits_{j=1}^{J} M_j w_1(j,z). \end{cases} \tag{11}$$

Since the incremental form can improve the accuracy of model effectively, we can get the incremental expression:

$$\begin{aligned} \hat{y}(k) = &\sum_{i=1}^{n+1} A_{1,i} y(k-i) + \sum_{i=1}^{m+1} B_{1,i} \Delta N_{\mathrm{eg}}(k-i) + \\ &\sum_{i=1}^{m+1} C_{1,i} \Delta u_{\mathrm{th}}(k-i) + \sum_{i=1}^{m+1} D_{1,i} \Delta u_{\mathrm{wg}}(k-i), \end{aligned} \tag{12}$$

where

$$\begin{cases} A_{1,1} = \begin{bmatrix} 1 & 0 \\ 0 & 1 \end{bmatrix} + a_1, \\ A_{1,i} = a_i - a_{i-1}, \ i = 2, \cdots, n, \\ A_{1,n+1} = -a_n, \\ B_{1,i} = b_i, \ i = 1, \cdots, m, \\ C_{1,i} = b_{i+m}, \ i = 1, \cdots, m, \\ D_{1,i} = b_{i+2m}, i = 1, \cdots, m, \\ A_{l,i} = A_{1,i+l-1} + \sum\limits_{j=1}^{l-1} A_{1,j} A_{l-j,i}, \\ \qquad i = 1, 2, \cdots, n, \\ B_{l,i} = B_{1,i+l-1} + \sum\limits_{j=2}^{l} A_{1,j-1} B_{l-j+1,i}, \\ \qquad i = 2, \cdots, m+1, \\ C_{l,i} = C_{1,i+l-1} + \sum\limits_{j=2}^{l} A_{1,j-1} C_{l-j+1,i}, \\ \qquad i = 2, \cdots, m+1, \\ D_{l,i} = D_{1,i+l-1} + \sum\limits_{j=2}^{l} A_{1,j-1} D_{l-j+1,i}, \\ \qquad i = 2, \cdots, m+1. \end{cases} \tag{13}$$

In general, the expanded centers are set to constant, so all the parameters of predictive equation are known in advance. Compare with physical modeling method, BPNN model is more suitable for controller designed by reason of its clear structure.

4.1.2 Model validation

The parameters of BPNN model are shown in follows: all of the input and output orders are $m = n = 3$. The number of input layer neurons is $I = 15$. The number of hidden layers neurons are $J = 10$, $H = 30$. In order to evaluate the linear BPNN model, a linear comparison model which is identified by identification toolbox is presented[27]. The two models are given under the same condition, and the curves of intake manifold pressure error and boost pressure error are showed in Fig. 9.

We can see from Fig. 9: the output errors of linear BPNN model are slightly smaller than the comparison model. In linear BPNN model, the average absolute errors of intake manifold pressure and boost pressure are 0.0027 and 0.0008 respectively, and in the comparison model, the average absolute errors of both pressures are 0.0040 and 0.0018.

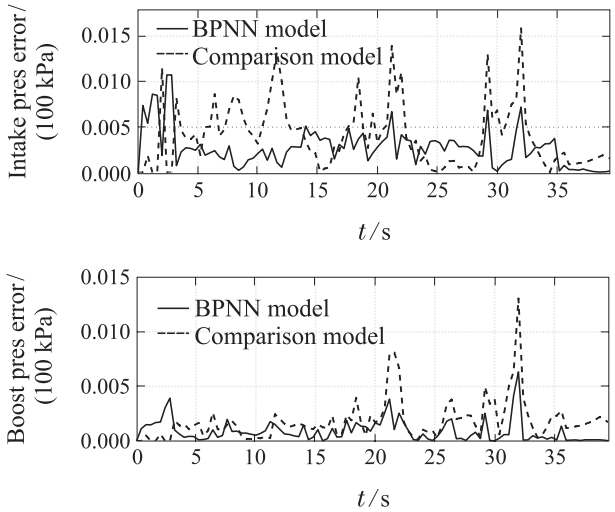

Fig. 9 The error of output data for validation

4.1.3 Predictive equation

We can get the predictive equation at step l:

$$\hat{y}(k+l) = \hat{y}_{\rm p}(k+l) + \sum_{i=0}^{l-1} B_{l-i,1}\Delta N_{\rm eg}(k+i) + \sum_{i=0}^{l-1} C_{l-i,1}\Delta u_{\rm th}(k+i) + \sum_{i=0}^{l-1} D_{l-i,1}\Delta u_{\rm wg}(k+i), \tag{14}$$

where

$$\hat{y}_p(k+l) = \sum_{i=1}^{n+1} A_{l+1,i}y(k-i) + \sum_{i=1}^{m} B_{l+1,i+1}\Delta N_{\rm eg}(k-i) + \sum_{i=1}^{m} C_{l+1,i+1}\Delta u_{\rm th}(k-i) + \sum_{i=1}^{m} D_{l+1,i+1}\Delta u_{\rm wg}(k-i). \tag{15}$$

Since the engine speed is treated as the system disturbance rather than a control variable, the future values of it have not to be calculated by controller. Hence, the values of $N_{\rm eg}$ at sampling time k, $k+1$, $\cdots$, $k+p-1$ are chosen as the same as the value of sampling time $k-1$. In addition, it is necessary to regulate the modeling error via E_1. Thereby, the predictive equation can be shown as

$$\hat{Y} = \hat{Y}_p + GU + G_3U_3 + E_1, \tag{16}$$

where

$$\begin{cases} \hat{Y} = [\hat{y}(k+1) \ \cdots \ \hat{y}(k+p)]^{\rm T}, \\ \hat{y}(k) = \begin{bmatrix} \hat{P}_{\rm im}(k) \\ \hat{P}_{\rm comp}(k) \end{bmatrix}, \\ \hat{Y}_p = [\hat{y}_p(k+1) \ \cdots \ \hat{y}_p(k+p)]^{\rm T}, \\ U = [\Delta u(k) \ \cdots \ \Delta u(k+p-1)]^{\rm T}, \\ \Delta u(k) = \begin{bmatrix} \Delta u_{\rm th}(k) \\ \Delta u_{\rm wg}(k) \end{bmatrix}, \\ U_3 = [\Delta N_{\rm eg}(k-1) \ \cdots \ \Delta N_{\rm eg}(k-1)]^{\rm T}, \\ E_1 = [y(k) - \hat{y}(k) \ \cdots \ y(k) - \hat{y}(k)], \\ G = \begin{bmatrix} \beta_{1,1} & O & \cdots & O \\ \beta_{2,1} & \beta_{1,1} & \cdots & O \\ \vdots & \vdots & \ddots & \vdots \\ \beta_{p,1} & \beta_{p-1,1} & \cdots & \beta_{1,1} \end{bmatrix}, \ \beta_{i,j} = \begin{bmatrix} C_{i,j} & D_{i,j} \end{bmatrix}, \\ G_3 = \begin{bmatrix} B_{1,1} & 0 & \cdots & 0 \\ B_{2,1} & B_{1,1} & \cdots & 0 \\ \vdots & \vdots & \ddots & \vdots \\ B_{p,1} & B_{p-1,1} & \cdots & B_{1,1} \end{bmatrix}, \ O = \begin{bmatrix} 0 & 0 \\ 0 & 0 \end{bmatrix}. \end{cases} \tag{17}$$

4.2 Model horizon optimization

In order to meet the desired torque, the tracking of intake manifold pressure and boost pressure, and the constraint of actuators should be taken into consideration. Therefore, the objective function is

$$J = \underset{U}{\rm minimize}\,[(Y_{\rm s} - \hat{Y})^{\rm T}\Gamma_{\rm y}(Y_{\rm s} - \hat{Y}) + U^{\rm T}\Gamma_{\rm u}U], \tag{18}$$

where

$$\begin{cases} Y_{\rm s} = [P_{\rm im}^{\rm s} \ P_{\rm comp}^{\rm s} \ \cdots \ P_{\rm im}^{\rm s} \ P_{\rm comp}^{\rm s}]^{\rm T}, \\ \Gamma_{\rm y} = {\rm diag}\{\Gamma_{{\rm y},1}, \Gamma_{{\rm y},2}, \cdots, \Gamma_{{\rm y},2\times p}\}, \\ \Gamma_{\rm u} = {\rm diag}\{\Gamma_{{\rm u},1}, \Gamma_{{\rm u},2}, \cdots, \Gamma_{{\rm u},2\times p}\}, \end{cases} \tag{19}$$

the constraints of throttle $u_{\rm th}$ and wastegate $u_{\rm wg}$ are

$$0 \leqslant u_{\rm th} \leqslant 100,\ 0 \leqslant u_{\rm wg} \leqslant 100. \tag{20}$$

The terms of $P^{\rm s}_{\rm im}$ and $P^{\rm s}_{\rm comp}$ are the desired intake pressure and boost pressure. p stands for the predictive horizon. When it is increasing, the performance of the control system improves, but the calculational burden increases sharply at the same time. $\Gamma_{\rm y}$ and $\Gamma_{\rm u}$ are weighting matrixes, which can adjust the control performance.

In this paper, the linear MPC is reduced to a quadratic programming (QP) problem, which is easy to be solved via QP function of MATLAB. The control sequence can be obtained by solving the related objective function, but only the previous element are applied to engine system.

Taken the linear predictive equation (16) into account, the objective function is transformed as

$$J = \underset{U}{\rm minimize}\,[\frac{1}{2}U^{\rm T}HU + f^{\rm T}U], \tag{21}$$

where

$$\begin{cases} H = 2 \times (G^{\rm T}\Gamma_{\rm y}G + \Gamma_{\rm u}), \\ f^{\rm T} = -2 \times (Y_{\rm s} - \hat{Y}_{\rm p} - G_3U_3 - E_1)^T\Gamma_{\rm y}G, \end{cases} \tag{22}$$

the constraints of throttle $u_{\rm th}$ and wastegate $u_{\rm wg}$ are

$$0 \leqslant u_{\rm th} \leqslant 100,\ 0 \leqslant u_{\rm wg} \leqslant 100. \tag{23}$$

5 Simulation results

The performance of the control system is tested in the environment of joint-simulation of MATLAB/Simulink and AMESim. The predictive horizon of linear MPC is $p = 4$. The weighting matrixes are $\Gamma_{\rm y} = {\rm diag}\{90, 6, 90, 6, 90, 6, 90, 6\}$, $\Gamma_{\rm u} = {\rm diag}\{10, 0.04, 10, 0.04, 10, 0.04, 10, 0.04\}$, respectively.

5.1 Fixed engine speed condition

Normally, the engine speed is required to be fixed, so we give the system a fixed engine speed at first. The engine speed is set to be 3500 r/min. The tracking curves of torque and pressures are shown in Figs.i0−11 respectively. The evolution of control input is shown in Fig. 12.

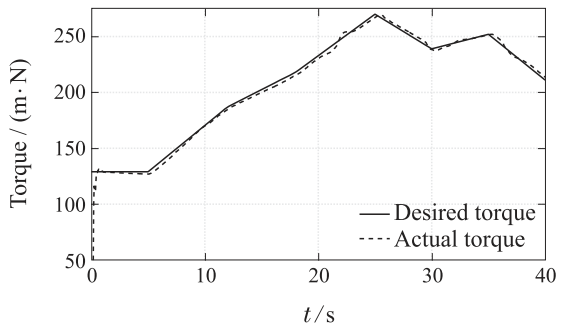

Fig. 10 The curves of torque

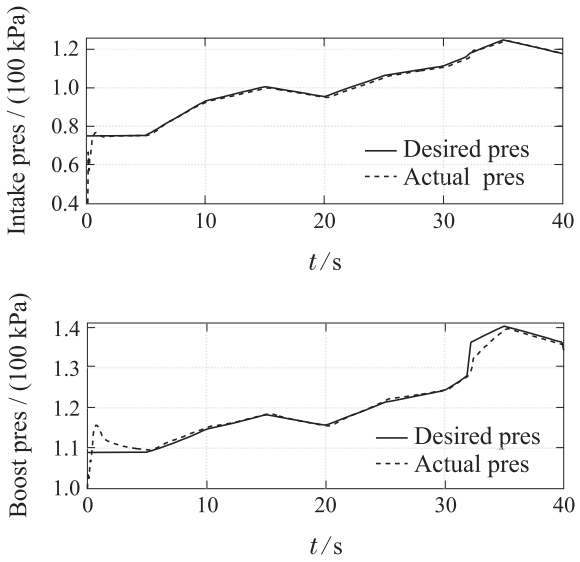

Fig. 11 The curves of pressures

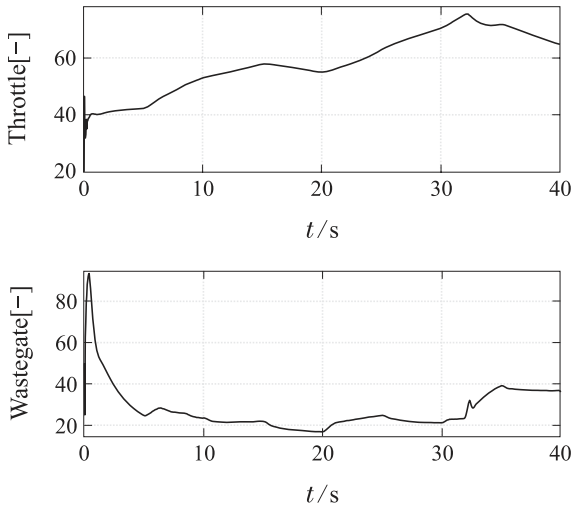

Fig. 12 The control input

5.2 Unfixed engine speed condition

In the actual operation of engine, it is necessary to accelerate and decelerate sometimes. Therefore, we verify the condition of unfixed engine speed in this section. The engine speed is shown in Fig. 13. The tracking curves of torque and pressures are shown in Figs. 14−15 respectively. The evolution of control input is shown in Fig. 16.

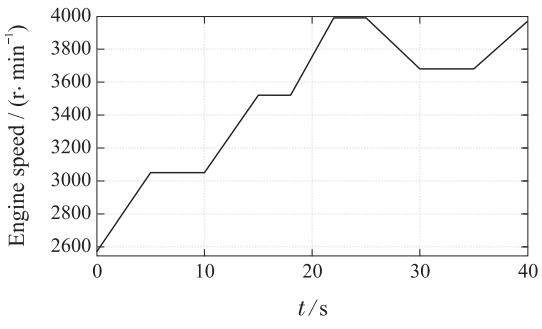

Fig. 13 The engine speed

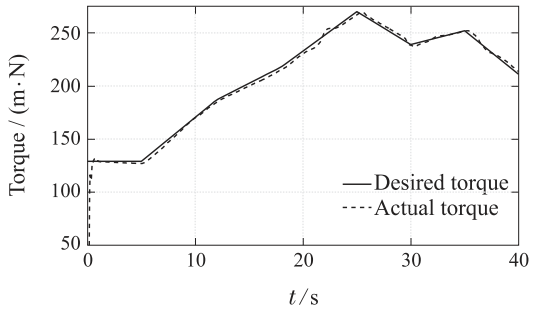

Fig. 14 The curves of torque

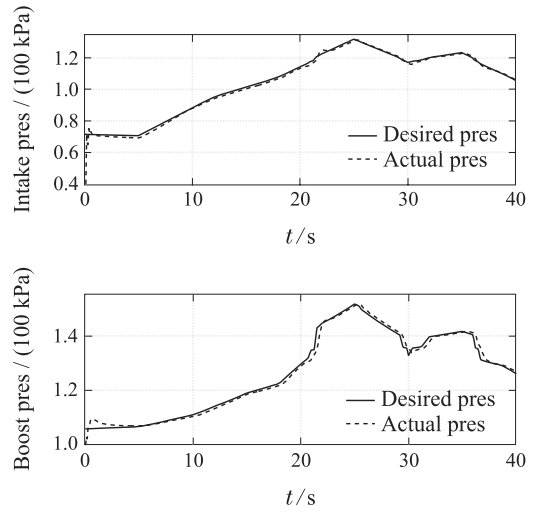

Fig. 15 The curves of pressures

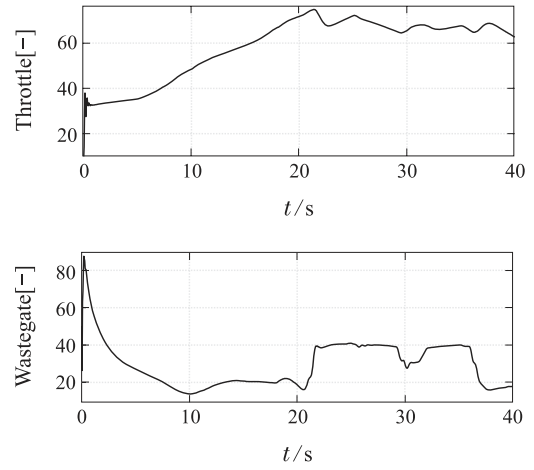

Fig. 16 The control input

We can see from the figures: no matter in fixed or unfixed speed conditions, proposed scheme works well. Since the linear controller unmodeled nonlinear dynamics of engine, the sharp change of desired pressures makes the tracking performance worse.

5.3 Controllers comparison

The proposed control scheme has been validated in both fixed engine speed condition and unfixed engine speed condition. In this section, the controller is compared with a double PID controller and a nonliear BPNN based MPC controller. This comparison is implemented on an Intel(R) Core(TM) i7–4790 CPU (3.60 GHz). The contrast curves of three controllers are shown in Fig. 17 and Fig. 18, and the computational time of them is recorded in Table 1. For the double PID controller, both the overshot and steady-state errors of the boost pressure are obvious and can't be eliminated. The overshot of boost pressure may be brought into by the large inertia of turbine. For nonlinear BPNN based MPC, in either the pressure tracking or torque tracking, its performance is the best. However, Table 1 reveals that the nonlinear MPC spends more optimization time by a factor of $\dfrac{0.696}{0.045} \approx 15.467$ for linear MPC. For linear BPNN based MPC, the tracking performance of it is slightly worse than nonlinear MPC, but the optimization time of it is reduced.

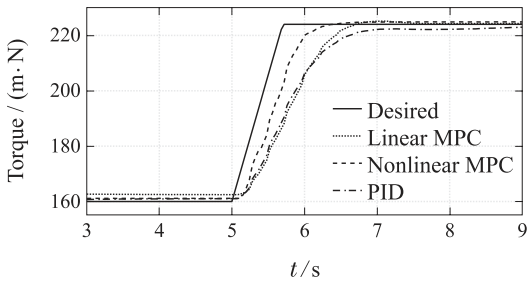

Fig. 17 The curves of torque

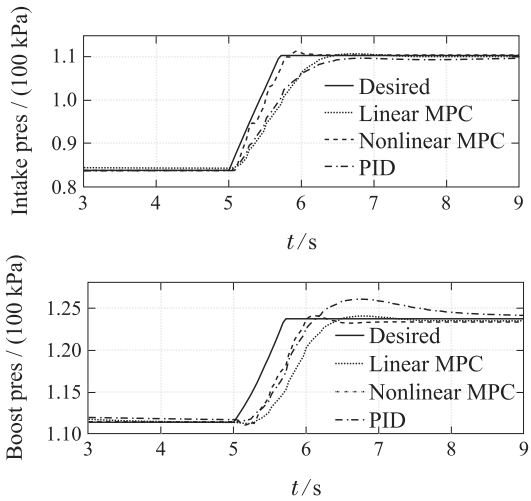

Fig. 18 The curves of pressures

Table 1 The comparison of computational time

MPC	Case			
	First	Second	Third	Average
LMPC	0.045 s	0.045 s	0.045 s	0.045 s
NMPC	0.710 s	0.682 s	0.695 s	0.696 s

6 Evaluation by RCP simulation

In this section, the linear MPC is evaluated by rapid control prototyping (RCP) platform based on

dSPACE. The implementation procedure is shown in Fig. 19. Firstly, a turbocharged gasoline engine model of AMESim is utilized as the plant, and it is downloaded to DS2211 through the combination of AMESim and Simulink. Then, the linear BPNN based MPC is established by embedded MATLAB function of Simulink, which is downloaded to DS1104. As QP function of MATLAB is an addition toolbox, which isn't suitable for dSPACE, dual algorithm is applied to solve the QP problem. Finally, the communication between DS2211 and DS1104 is achieved by their build-in AD/DA module. In order to observe the results of RCP experiment, the ControlDesk software is chosen to display the graphs and collect data.

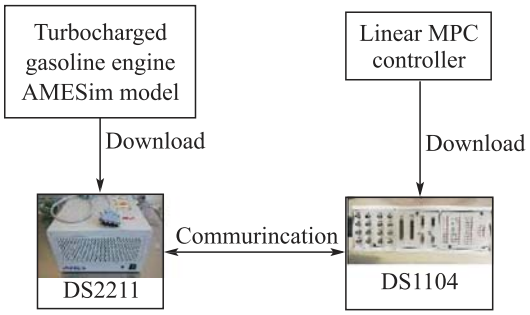

Fig. 19 The RCP implement procedure

The RCP experiment is carried out in unfixed engine speed condition. The engine speed is shown in Fig. 20. The tracking curves of torque and pressures are shown in Figs. 21−22 respectively. The evolution of control input is shown in Fig. 23.

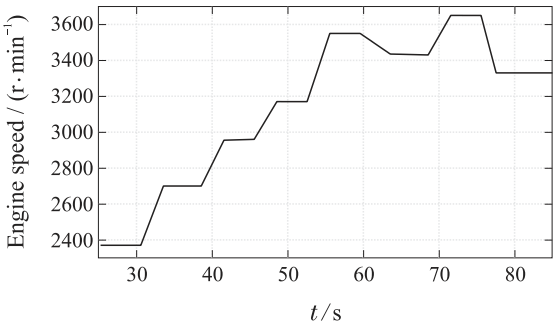

Fig. 20 The engine speed

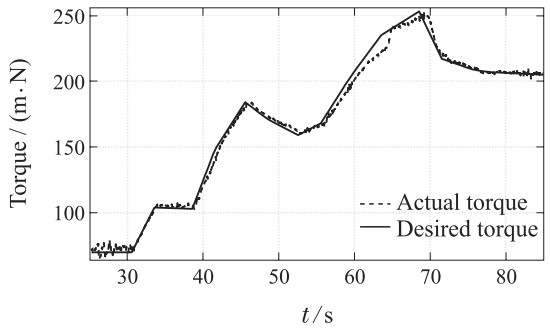

Fig. 21 The curves of torque

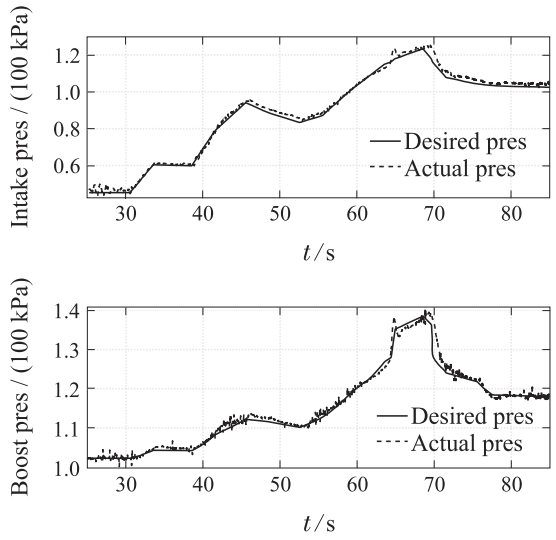

Fig. 22 The curves of pressures

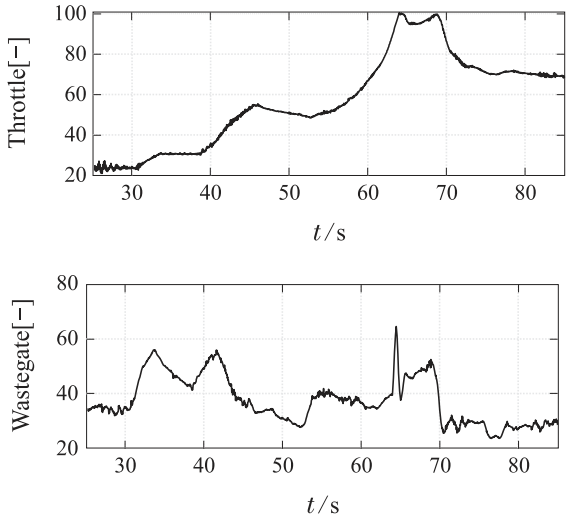

Fig. 23 The control input

As shown in figures, the actual output of the plant can track the desired values well. It is known that: BPNN based linear MPC can not only achieve better performance but also ensure real-time computation.

7 Conclusions

In this paper, a BPNN based model predictive controller is proposed for the coordinated control of throttle and wastegate in turbocharged gasoline engine airpath system. Firstly, a BPNN predictive model is obtained to predict the future dynamics of intake manifold pressure and boost pressure. Secondly, the predictive model is linearized by Taylor expansion. Thirdly, a linear MPC is designed to track the desired pressures so as to meet the purpose of torque tracking. Finally, the off-line simulation results and the rapid control prototyping experiment demonstrate that the proposed control scheme can achieve the control requirements.

References:

[1] WANG Y N, SHEN Y P, MENG B M, et al. Electronic control for gasoline automotive engine: state of the art and perspective [J]. *Journal of Control Theory and Applications*, 2015, 32(4): 432 – 447.

[2] KASSERIS E P, HEYWOOD J B. Comparative analysis of automotive powertrain choices for the next 25 years [J]. *SAE Technical Paper*, 2007, 116: 626 – 648.

[3] HADEF J E, COLIN G, CHAMAILLARD Y, et al. Turbocharged SI engine models for control [C] //*Proceedings of the 11th International Symposium on Advanced Vehicle Control*. Seoul, Korea: AVEC'12, 2012.

[4] KALABIC U, KOLMANOVSKY I, BUCKLAND J. Reference and extended command governors for control of turbocharged gasoline engines based on linear models [C] //*IEEE International Conference on Control Applications*. Denver, USA: IEEE, 2011: 319 – 325.

[5] KAINIK A Y, BUCKLAND J H, FREUDENBERG J S. Electronic throttle and wastegate control for turbocharged gasoline engines [C] //*Proceedings of the 2005 American Control Conference*. Portland, USA: IEEE, 2005: 4434 – 4439.

[6] MOULIN P, CHAUVIN J, YOUSSEF B. Modelling and control of the air system of a turbocharged gasoline engine [J]. *IFAC Proceedings Volumes*, 2008, 41(2): 8487 – 8494.

[7] MOULIN P, CHAUVIN J. Modeling and control of the air system of a turbocharged gasoline engine [J]. *Control Engineering Practice*, 2011, 19(3): 287 – 297.

[8] NGUYEN T A, LAUBER J, DAMBRINE M. Robust H_∞ control design for switching uncertain system: Application for turbocharged gasoline air system control [C] //*IEEE Conference on Decision and Control*. Maui, USA: IEEE, 2012: 4265 – 4270.

[9] NGUYEN A T, LAUBER J. Multi-objective control design for turbocharged spark ignited air system: a switching Takagi-Sugeno model approach [C] //*2013 American Control Conference*. Washington, USA: IEEE, 2013: 2866 – 2871.

[10] ZHOU X. *Data-driven based turbocharged gasoline engine air path predictive control* [D]. Jilin: University of Jilin, 2016.

[11] QIU Z, JANKOVIC M, SANTILLO M. Composite adaptive internal model control and its application to boost pressure control of a turbocharged gasoline engine [J]. *IEEE Transactions on Control Systems Technology*, 2015, 23(6): 2306 – 2315.

[12] COLIN G, CHAMAILLARD Y, BLOCH G, et al. Exact and linearized neural predictive control: a turbocharged si engine example [J]. *Journal of Dynamic Systems, Measurement, and Control*, 2007, 129(4): 527 – 533.

[13] QIU Z, SUN J, JANKOVIC M. Nonlinear internal model controller design for wastegate control of a turbocharged gasoline engine [J]. *Control Engineering Practice*, 2016, 46: 105 – 114.

[14] COLIN G, CHAMAILLARD Y, BLOCH G, et al. Neural control of fast nonlinear systems-application to a turbocharged SI engine With VCT [J]. *IEEE Transactions on Neural Networks*, 2007, 18(4): 1101 – 1114.

[15] KARNIK A Y, BUCKLAND J H, FREUDENBERG J S. Electronic throttle and wastegate control for turbocharged gasoline engines [C] //*American Control Conference*. Portland, USA: IEEE, 2005: 4434 – 4439.

[16] SANTILLO M, KARNIK A. Model predictive controller design for throttle and wastegate control of a turbocharged engine [C] //*American Control Conference*. Washington, USA: IEEE, 2013: 2183 – 2188.

[17] DEFENG H, LEI W, JIN S. On stability of multiobjective NMPC with objective prioritization [J]. *Automatica*, 2015, 57(2015): 189 – 198.

[18] KALOGIROU S A. Artificial neural networks in renewable energy systems applications: a review [J]. *Renewable and Sustainable Energy Reviews*, 2001, 5(4): 373 – 401.

[19] BOUVENOT J B, ANDLAUER B. Gas stirling engine μCHP boiler experimental data driven model for building energy simulation [J]. *Energy and Buildings*, 2014, 84: 117 – 131.

[20] TAYARANI-BATHAIE S S, VANINI Z N S, KHORASANI K. Dynamic neural network-based fault diagnosis of gas turbine engines [J]. *Neurocomputing*, 2014, 125(3): 153 – 165.

[21] AMOZEGAR M, KHORASANI K. An ensemble of dynamic neural network identifiers for fault detection and isolation of gas turbine engines [J]. *Neural Networks*, 2016, 76(2016): 106 – 121.

[22] TAHBOUB K K, BARGHASH M, ARAFEH M, et al. An ANN-GA framework for optimal engine modeling [J]. *Mathematical Problems in Engineering*, 2016, (2016): 1 – 8.

[23] SHIVAKUMAR, PAI P S, RAO B R S. Artificial neural network based prediction of performance and emission characteristics of a variable compression ratio CI engine using WCO as a biodiesel at different injection timings [J]. *Applied Energy*, 2011, 88(7): 2344 – 2354.

[24] CAY Y. Prediction of a gasoline engine performance with artificial neural network [J]. *Fuel*, 2013, 111(3): 324 – 331.

[25] GÉRARD B, DENOEUX T. The adaptive control using BP neural networks for a nonlinear servo-motor [J]. *Journal of Control Theory and Applications*, 2008, 6(3): 273 – 276.

[26] MO L. Study on surface settlement prediction technique based on BP neural network [C] //*The 6th International Conference on Intelligent Systems Design and Engineering Applications (ISDEA)*. Guiyang: IEEE, 2015: 760 – 762.

[27] ZHAO D, LIU C, STOBART R, et al. An explicit model predictive control framework for turbocharged diesel engines [J]. *IEEE Transactions on Industrial Electronics*, 2014, 61(7): 3540 – 3552.

作者简介:

陈　欢　(1991–), 女, 硕士研究生, 目前研究方向为发动机建模与控制, E-mail: 13194395391@163.com;

胡云峰　(1983–), 男, 副教授, 目前研究方向为发动机建模与控制、非线性控制方法在汽车控制系统设计中的应用, E-mail: huyf@jlu.edu.cn;

于树友　(1974–), 男, 副教授, 目前研究方向为模型预测控制及其在汽车控制中的应用, E-mail: yushuyou@126.com;

孙鹏远　(1974–), 男, 高级工程师, 目前研究方向为汽车发动机电子控制系统设计, E-mail: sunpengyuan@126.com;

陈　虹　(1963–), 女, 教授, 目前研究方向为为模型预测控制、鲁棒控制、非线性控制以及其在汽车控制系统中的应用, E-mail: chenh@jlu.edu.cn.